

Dirty Weyl semimetals: stability, phase transition and quantum criticality

Soumya Bera,¹ Jay D. Sau,² and Bitan Roy²

¹Max-Planck-Institut für Physik Komplexer Systeme, 01187 Dresden, Germany

²Condensed Matter Theory Center, Department of Physics,
University of Maryland, College Park, MD 20742, USA

(Dated: September 16, 2022)

We study the stability of three-dimensional incompressible Weyl semimetals in the presence of random quenched charge impurities. Using numerical analysis and scaling theory we show that in the presence of sufficiently weak randomness (i) Weyl semimetal remains stable, while (ii) the double-Weyl semimetal gives rise to compressible diffusive metal where the mean density of states at vanishing energy is finite. At stronger disorder, Weyl semimetal undergoes a quantum phase transition and enter into a metallic phase. Mean density of states at zero energy serves as the order parameter and displays single-parameter scaling across such disorder driven phase transition. We numerically determine various exponents at the critical point, which appear to be insensitive to the number of Weyl pairs, and also extract the extent of the quantum critical regime at finite energy.

PACS numbers: 71.30.+h, 05.70.Jk, 11.10.Jj, 71.55.Ak

Introduction: Over the span of last few years the horizon of topological phases of matter has been extended beyond the gapped states [1, 2] and now includes various gapless systems as well [3, 4]. Three-dimensional Weyl semimetal (WSM), constituted by the so called Weyl nodes that act as (anti)monopoles for *Berry flux* in the reciprocal space, is the prime example of such non-insulating systems. As the hallmark signature of topologically nontrivial ground state, WSMs also accommodate gapless surface states that can give rise to peculiar electro-magnetic responses, such as, the anomalous Hall and the chiral-magnetic effects [5]. While the gapped topological phases are expected to be robust against sufficiently weak randomness, stability of their gapless counterpart against disorder demands careful investigation and constitutes the central theme of this Letter.

Recent time has witnessed the discovery of WSMs in a number of inversion-asymmetric systems, such as TaAs [6–8], NbAs [9], TaP [10]. Various other proposals for WSMs, for example, include anti-ferromagnetically ordered pyrochlore iridates [11], multilayer configuration of topological and regular insulators [12, 13], magnetically doped topological insulators [14]. The monopole charge of the Weyl nodes in these systems is ± 1 . Nevertheless, HgCr₂Se₄ [15], SrSi₂ [16] are expected to host Weyl nodes with monopole charge ± 2 , dubbed as the double-WSM. The topological invariant and the enclosed Berry flux in double-WSM is twice that in a WSM, and consequently the one-dimensional chiral surface states in the former system possess a two-fold degeneracy. Although electro-magnetic responses in Weyl materials are reasonably well understood by now [5], stability of these incompressible topological semimetals in the presence of quenched randomness is yet to be explored and settled. This is the quest that has recently culminated in a surge of analytical [17–26] and numerical [27–34] works and we pursue it here for WSM and double-WSM, using numerical and analytical methods.

We address the stability of these two systems against

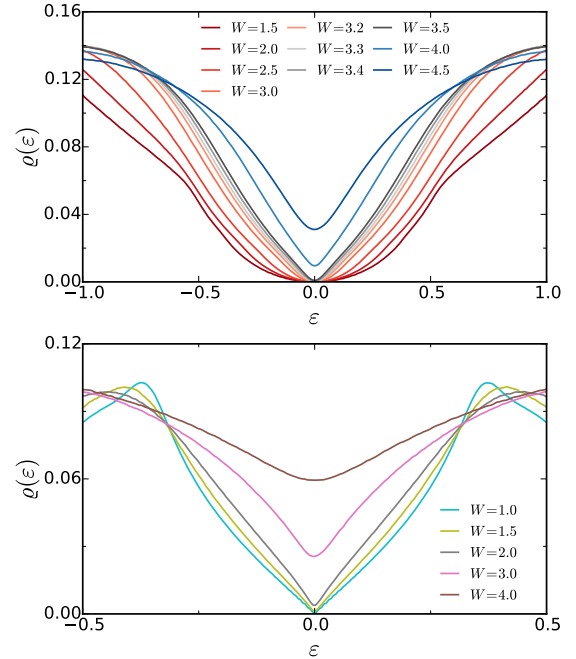


FIG. 1. (Color online) Mean DOS in (a) WSM and (b) double-WSM. Respectively in these two systems the mean DOS scales as $q(\varepsilon) \sim |\varepsilon|^2$ and $|\varepsilon|$. WSM remains stable up to $W_c = 3.5 \pm 0.1$, beyond which the mean DOS at $\varepsilon = 0$, $q(0)$ is finite, and the system becomes a CDM. The double-WSM visibly turns into a CDM for weak enough disorder $W \sim 1.0$.

random quenched charge impurities by analyzing the mean density of states (DOS) at the zero energy, where non-degenerate valence and conduction band touch each other. Our central results are: (a) While WSMs are stable [21, 29, 31, 33, 34], the double-WSM undergoes a BCS-like weak coupling instability towards the formation of a compressible diffusive metal (CDM), where the mean DOS at zero energy is finite, for weak disorder [see Fig. 1]. (b) WSMs undergo a disorder driven quantum

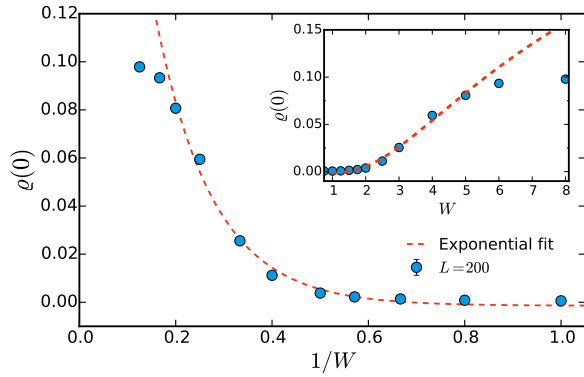


FIG. 2. (Color online) Mean DOS at zero energy $\rho(0)$ in double-WSM as a function of $1/W$. Inset: scaling of $\rho(0)$ with W . The dotted lines correspond to the BCS scaling.

phase transition (QPT), beyond which the system becomes a CDM. This situation is qualitatively similar to the one for three-dimensional dirty Dirac semimetal [17, 18, 20, 25, 28, 30, 32]. (c) Across the WSM-CDM transition mean DOS display single-parameter scaling and within our numerical accuracy the critical exponents at such itinerant quantum critical point (QCP) appear to be insensitive to the number of Weyl pairs (N_W) (Table I).

Model: A paradigmatic two-band model

$$H_W = \sum_{\mathbf{k}} \Psi_{\mathbf{k}}^\dagger [N_1(\mathbf{k})\sigma_1 + N_2(\mathbf{k})\sigma_2 + N_3(\mathbf{k})\sigma_3] \Psi_{\mathbf{k}}, \quad (1)$$

can describe different members of the Weyl family, where σ 's are the standard Pauli matrices, and $\Psi_{\mathbf{k}}$ is a two component spinor. Fermionic annihilation operators $c_{s,\mathbf{k}}$ with spin-projections $s = \uparrow, \downarrow$ and wave vector \mathbf{k} , constitute the spinor basis $\Psi_{\mathbf{k}}^\top = (c_{\uparrow,\mathbf{k}}, c_{\downarrow,\mathbf{k}})$.

This model supports a WSM upon choosing $N_1(\mathbf{k}) = t \sin(k_1 a)$, $N_2(\mathbf{k}) = t \sin(k_2 a)$, $N_3^1(\mathbf{k}) = t \cos(k_3 a)$ and $N_3^2(\mathbf{k}) = t'[2 - \cos(k_1 a) - \cos(k_2 a)]$, where a is the lattice spacing and $N_3(\mathbf{k}) = N_3^1(\mathbf{k}) + N_3^2(\mathbf{k})$. On a cubic lattice with periodic boundary in each direction, the above Hamiltonian translates into a tight-binding model

$$H = \sum_{\mathbf{r}} \left[\frac{t}{2} \Psi_{\mathbf{r}}^\dagger \sigma_3 \Psi_{\mathbf{r}+\hat{e}_3} + \sum_{j=1,2} \Psi_{\mathbf{r}}^\dagger \left[\frac{it}{2} \sigma_j - \frac{t'}{2} \sigma_3 \right] \Psi_{\mathbf{r}+\hat{e}_j} + H.c \right] + \sum_{\mathbf{r}} \Psi_{\mathbf{r}}^\dagger [2t' \sigma_3 + V(\mathbf{r})] \Psi_{\mathbf{r}}, \quad (2)$$

where $\Psi_{\mathbf{r}}^\top = (c_{\mathbf{r},\uparrow}, c_{\mathbf{r},\downarrow})$, and $c_{\mathbf{r},s}$ is electronic annihilation operator at site \mathbf{r} with spin projection $s = \uparrow, \downarrow$. Nearest-neighbor sites are connected by the unit vectors \hat{e}_j , for $j = 1, 2, 3$. The Weyl nodes are located at $\mathbf{k} = (0, 0, \pm \frac{\pi}{2a})$. Excitations in the vicinity of these two points are respectively described by left and right chiral fermions. The effect of random impurities is captured by $V(\mathbf{r})$, distributed uniformly and independently within $[-\frac{W}{2}, \frac{W}{2}]$. Effective low energy theory, derived by linearizing the dispersion near the Weyl nodes, reads as

$$H_1 = \Psi_\tau^\dagger [-iv(\sigma_1 \partial_1 + \sigma_2 \partial_2 + \tau \sigma_3 \partial_3) + V(\mathbf{r})] \Psi_\tau, \quad (3)$$

| N_W | W_c | z | ν_M | ν_W | ν_L |
|-------|---------------|-----------------|-----------------|-----------------|----------------|
| 1 | 3.5 ± 0.1 | 1.43 ± 0.05 | 1.1 ± 0.1 | 0.8 ± 0.14 | 1.1 ± 0.1 |
| 4 | 2.1 ± 0.1 | 1.48 ± 0.03 | 1.06 ± 0.18 | 0.65 ± 0.12 | 1.16 ± 0.1 |

TABLE I. Comparison of critical disorder for WSM-CDM QPT (W_c), dynamic critical exponent (z), and correlation length exponent (ν) extracted from the scaling of mean DOS (see text) for WSM with $N_W = 1, 4$ [35]. Exponents are reasonably close to the ones for Dirac fermions [28, 30, 32].

where $v \sim ta$, $\tau = \pm$ represent left and right chiral sectors, respectively. For $t' = 0$ three new pairs of Weyl nodes ($N_W = 4$) appear at $\mathbf{k} = \frac{\pi}{a}(0, 1, \pm \frac{1}{2})$, $\frac{\pi}{a}(1, 0, \pm \frac{1}{2})$, $\frac{\pi}{a}(1, 1, \pm \frac{1}{2})$ and $N_3^2(\mathbf{k})$ plays the role of *Wilson mass*.

A double-WSM can also be realized from Eq. (1) by taking $N_1(\mathbf{k}) = t_1[\sin(k_1 a) - \sin(k_2 a)]$ and $N_2(\mathbf{k}) = t_1 \cos(k_1 a) \cos(k_2 a)$, while keeping $N_3^1(\mathbf{k})$ and $N_3^2(\mathbf{k})$ unaltered. Following the same spirit, we implement the corresponding tight-binding model in a cubic lattice, with periodic boundary in each direction [35]. The left and the right chiral fermions reside near $\mathbf{k} = (\frac{\pi}{2a}, \frac{\pi}{2a}, \pm \frac{\pi}{2a})$, respectively. The low-energy theory for a double-WSM in the presence of random charge impurities is

$$H_2 = \Psi_\tau^\dagger \left[\sigma_1 \frac{\partial_2^2 - \partial_1^2}{2m} - \sigma_2 \frac{2\partial_1 \partial_2}{2m} - iv\tau \sigma_3 \partial_z + V(\mathbf{r}) \right] \Psi_4 \quad (4)$$

where $m^{-1} \sim t_1 a^2$. We here set $t = t' = t_1 = 1 = a$.

Method: Mean DOS is numerically evaluated using the kernel polynomial method [28, 36]. We typically take ~ 30 disorder realization to minimize the residual statistical error, which is quite small in large system ($L = 220$) due to the self-averaging nature of mean DOS. We usually take 4096 Chebyshev moments and few (~ 8) trace vectors to calculate mean DOS, which is sufficient for the convergence of global quantities such as mean DOS.

Scaling: To understand the scaling of mean DOS and the stability of WSMs in the presence of impurities, we use both analytical and numerical approaches. Performing the disorder averaging, assuming a Gaussian white noise distribution with zero mean, i.e., $\langle \langle V(\mathbf{r})V(\mathbf{r}') \rangle \rangle = \Delta \delta^3(\mathbf{r} - \mathbf{r}')$, we obtain the replicated Euclidean action

$$\bar{S}_n = \int d^3x dt \Psi_a^\dagger [\partial_t + \tilde{H}_n] \Psi_a(x, t) - \frac{\Delta}{2} \int d^3x dt dt' (\Psi_a^\dagger \Psi_a)_{(x,t)} (\Psi_b^\dagger \Psi_b)_{(x,t')}, \quad (5)$$

for WSM ($n = 1$) and double-WSM ($n = 2$), where a, b are replica indices and \tilde{H}_n corresponds to the Hamiltonian from Eqs. (3) and (4) in the clean limit.

The scale invariance of physical observables (v and m) dictates the following space-time(imaginary) scaling ansatz: $(x, y) \rightarrow e^{l/n}(x, y)$, $z \rightarrow e^l z$ and $t \rightarrow e^l t$, accompanied by the rescaling of fermionic field $\Psi \rightarrow e^{-(\frac{1}{n} + \frac{1}{2})l} \Psi$, where $l \sim \log \frac{L}{a}$ is the scaling parameter. The scaling dimension of disorder coupling is, therefore,

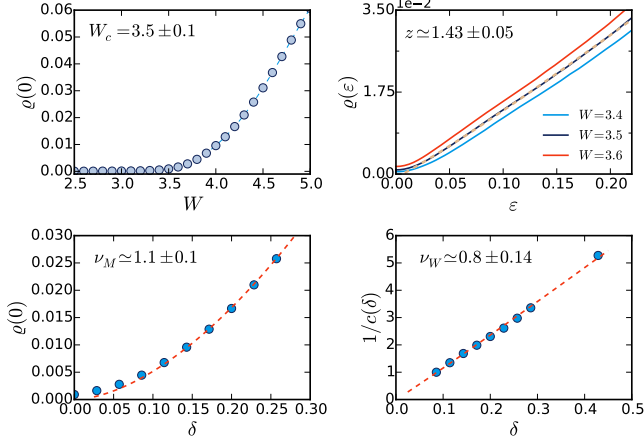


FIG. 3. (Color online) (a) Mean DOS at zero energy $\rho(0)$ vs. disorder (W), (b) mean DOS $\rho(\varepsilon)$ vs. ε for $W = 3.4, 3.5, 3.6$. (c) $\rho(0)$ vs. δ , where $\delta = (W - W_c)/W_c$, and (d) $c(\delta)^{-1}$ vs. δ , where $c(\delta) = \delta^{(z-1)d\nu}$, for WSM with $N_W = 1$, assuming $W_c = 3.5$. Similar analysis has been performed for WSM with $N_W = 4$ [35]. Results are summarized in Table I.

$[\Delta] = 1 - \frac{2}{n}$. Hence, sufficiently weak disorder is an *irrelevant* (since $[\Delta] = -1$) and a *marginally relevant* (since $[\Delta] = 0$) perturbation in WSM and double-WSM, respectively [35]. Therefore, (double-)WSM is expected to be (un)stable in the presence of weak randomness.

Notice that $[\Delta] \equiv 2z - d$, where d is dimensionality of the system and z is the dynamic critical exponent, together governing the scaling of mean DOS $\rho(\varepsilon) \sim |\varepsilon|^{d/z-1}$. Therefore, with $z = 1$ and $\frac{3}{2}$, $\rho(\varepsilon) \sim |\varepsilon|^2$ and $|\varepsilon|$, respectively for WSM and double-WSM, in complete agreement with our numerical findings, see Fig. 1.

Stability: WSM remains stable for weak disorder ($W \lesssim 3.5$) and mean DOS at zero energy $\rho(0) = 0$, in agreement with our scaling theory [Fig. 1(a)]. However, for strong disorder WSM appears to undergo a QPT and enter into the CDM phase, where $\rho(0)$ is finite. This observation is in agreement with various field theoretic [17–21, 25], and numerical analyses for three-dimensional Dirac [27, 28, 30, 32] and Weyl [31, 33, 34] fermion. We will delve into the nature of such QPT in the next section.

The scaling analysis suggests a BCS-like instability of double-WSM towards the formation of CDM for infinitesimal randomness. Available data of $\rho(0)$ for double-WSM in a finite system, on the other hand, suggest a putative threshold value of disorder ($W_{th} \approx 1$) beyond which $\rho(0)$ is visibly finite [Fig. 1(b)]. To examine whether the observed finite- $\rho(0)$ is a consequence of a $W = 0^+$ instability, we compare $\rho(0)$ as a function of $1/W$ (Fig. 2). It is evident that larger systems are required to pin the exponential onset of $\rho(0)$ for sufficiently weak W , as $W_{th} \sim 1/\log(L)$. Still, $\rho(0)$ depicts a overall good agreement with exponential decrease with $1/W$. In addition, $\rho(0)$ fits very well with the celebrated BCS scaling form $\rho(0) \sim \exp(-\lambda/W)$, with $\lambda = 10.7 \pm 0.4$ [Fig. 2(Inset)]. Notice that $\rho(0)$ starts to deviate from

BCS scaling for $W > 5.0$ and falls below the exponential line. Such behavior can be attributed to the well-known Anderson transition of a three-dimensional metal, across which the mean DOS does not display critical behavior, but decreases monotonically [30]. We anticipate that for $W > 5.0$ the double-WSM falls within the basin of attraction of metal-insulator (Anderson) critical point.

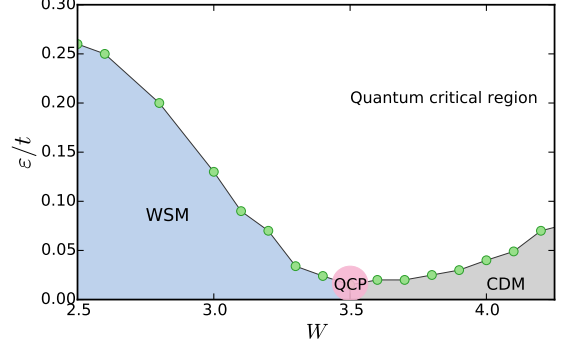


FIG. 4. (Color online) Phase diagram of dirty WSM with $N_W = 1$ and $L = 220$, as a function of energy (ε). The crossover between the WSM and critical regime occurs where $\rho(\varepsilon)$ ceases to scale as $|\varepsilon|^2$. At the boundary between the critical regime and CDM, $\rho(\varepsilon)$ deviates from $|\varepsilon|$ -scaling.

Critical exponents: Next we explore the critical behavior of pure disorder driven QPT in WSM. Our results are summarized in Table I for $N_W = 1$ and 4. Below we only quote the results for WSM with $N_W = 1$. Fig. 3(a) suggest that $\rho(0)$ can serve as a order parameter across the WSM-CDM QPT, which is zero and finite in these two phases, respectively, and we estimate $W_c = 3.5 \pm 0.1$.

Total number of states $\mathcal{N}(\varepsilon, L)$ below the energy ε in a system of linear size L is proportional to L^d and in general a function of two dimensionless variables L/ξ and $\varepsilon/\varepsilon_0$. $\xi(\sim \delta^{-\nu})$ is the correlation length that diverges and $\varepsilon_0(\sim \delta^{\nu z})$ is the corresponding energy scales that, in contrast, vanishes as one approaches the QCP ($\delta \rightarrow 0$), where $\delta = (W - W_c)/W_c$ measures the deviation from the QCP (W_c) and ν is the correlation length exponent [37, 38]. With these notions, we can write

$$\mathcal{N}(\varepsilon, L) = (L/\xi)^d \mathcal{G}(\varepsilon \delta^{-\nu z}, L^{1/\nu} \delta), \quad (6)$$

where \mathcal{G} is an unknown scaling function. From the definition of mean DOS $\rho(\varepsilon, L) = L^{-d} d\mathcal{N}(\varepsilon, L)/d\varepsilon$, we then arrive at the scaling ansatz for mean DOS

$$\rho(\varepsilon, L) = \delta^{\nu(d-z)} \mathcal{F}(|\varepsilon| \delta^{-\nu z}, L^{1/\nu} \delta), \quad (7)$$

after accounting the particle-hole symmetry, i.e., $\rho(\varepsilon, L) = \rho(-\varepsilon, L)$, where \mathcal{F} is the scaling function.

First we consider a sufficiently large system ($L = 220$), so that the finite size effects are negligibly small and the L -dependence in Eq. (7) can be ignored. At the QCP ($\delta = 0$), the δ -dependence of $\rho(\varepsilon)$ must cancel out, demanding $F(x) \sim x^{\frac{d}{z}-1}$, and therefore $\rho(\varepsilon) \sim |\varepsilon|^{\frac{d}{z}-1}$. From Fig. 3(b) we obtain $z = 1.43 \pm 0.05$ for $N_W = 1$.

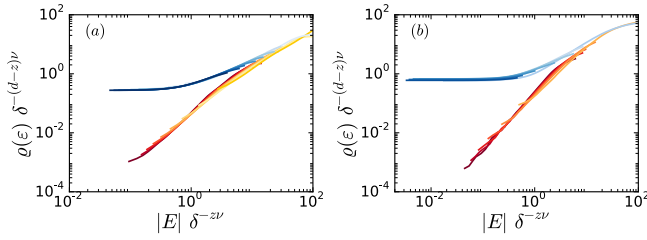


FIG. 5. (Color online) Single parameter scaling of mean DOS in WSM with (a) $N_W = 1$, (b) $N_W = 4$, and $L = 200$. Top (bottom) branch corresponds to CDM (WSM). Plots are obtained for $(W_c, z, \nu) = (3.5, 1.43, 1.1)$ and $(2.1, 1.48, 1.06)$ for $N_W = 1$ and 4, respectively.

In the metallic phase, the mean DOS at zero energy $\rho(0)$ is finite and serves as the order parameter. In this regime $\rho(0) \sim \delta^{(d-z)\nu}$ and one can identify $(d-z)\nu$ as the order parameter exponent (β). However, such power law dependence of $\rho(0)$ is valid when $\xi \ll L$. Therefore, we fit $\rho(0)$ as $\delta^{(d-z)\nu}$ for $\delta \geq 0.06$ [Fig. 3(c)], and obtain $\nu_M = 1.1 \pm 0.1$ for $N_W = 1$, where ν_M is the correlation length exponent extracted from the metallic phase.

In WSM, the mean DOS scales as $\rho(\varepsilon) \sim c(\delta)^{-1}|\varepsilon|^{d-1}$, so that we recover $\rho(\varepsilon) \sim |\varepsilon|^2$ for $d = 3$, where ν_W is the correlation length exponent extracted from the WSM phase and $c(\delta) \sim \delta^{(z-1)d\nu_W}$. However, it should be noted that for $W < W_c$, mean DOS displays a smooth crossover from $|\varepsilon|^2$ (for small ε) to $|\varepsilon|$ (for large ε) dependence. Therefore, estimation of ν_W depends crucially on the range over which we attempt to fit $\rho(\varepsilon) \sim |\varepsilon|^2$, and accuracy of ν_W can be questioned. Nevertheless, by fitting the coefficient of $|\varepsilon|^2$ with $c(\delta)^{-1}$ [Fig. 3(d)], we obtain $\nu_W = 0.8 \pm 0.14$, for $N_W = 1$.

Critical regime: The crossover from the quadratic (at small energy) to the linear (for higher energies) scaling of $\rho(\varepsilon)$ allows us to estimate the boundary between the WSM and the critical regime at finite energy when $W < W_c$. For sufficiently weak disorder, $\rho(\varepsilon) \sim |\varepsilon|^2$ over a wide range of energy. As the randomness is gradually increased (but still $W < W_c$), more and more degrees of freedom need to be integrated out (in the spirit of renormalization group) to wash out the effect of disorder from the system. Consequently, the energy window over which $\rho(\varepsilon) \sim |\varepsilon|^2$ gets reduced and the region where $\rho(\varepsilon) \sim |\varepsilon|$ increases, with increasing disorder. With this notion we numerically estimate the crossover boundary between the WSM and the critical regime at finite energy (Fig. 4). When $W = W_c$, the mean DOS displays a $|\varepsilon|$ -linear dependence over the entire energy range ($|\varepsilon| < 0.5$). For $W > W_c$, $|\varepsilon|$ -linear behavior of $\rho(\varepsilon)$ ceases at finite energy, defining the boundary between the CDM and the critical regime, and gives rise to a finite $\rho(0)$ (Fig. 4).

Data collapse: Next we show that $\rho(\varepsilon)$ display a single parameter scaling across the WSM-CDM QPT. Motivated by Eq. (7), we compare $\rho(\varepsilon)\delta^{-(d-z)\nu}$ and $|\varepsilon|\delta^{-z\nu}$ for $L = 220$ and $N_W = 1$ [Fig. 5(a)]. Neglecting the high energy part of spectrum ($|\varepsilon| > 0.5$) outside the weyl cones

and extreme small energy ($|\varepsilon| < 10^{-2}$) where numerical accuracy is small, we find that all data from Fig. 1(a) collapse onto two separate branches, associated with the CDM and the WSM phases, as shown in Fig. 5(a).

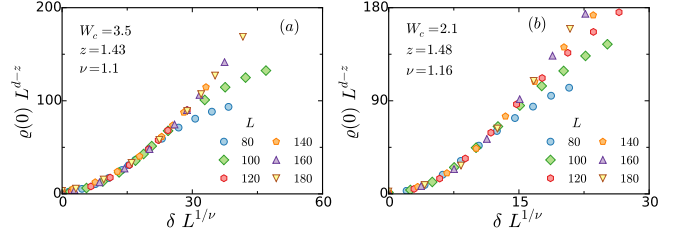


FIG. 6. (Color online) Finite size data collapse of $\rho(0, L)$ for (a) $N_W = 1$, and (b) $N_W = 4$. While the data collapse is quite good for small δ , it deviates from single-parameter scaling, due to the Anderson transition at strong disorder.

Finally, we delve into the finite size data collapse for the mean DOS at $\varepsilon = 0$ and estimate ν independently. Setting $\varepsilon = 0$ in Eq. (7), we obtain $\rho(0, L) = L^{z-d}\mathcal{F}(0, \delta L^{1/\nu})$. An excellent data collapse is achieved by comparing $\rho(L, 0)L^{d-z}$ vs. $\delta L^{1/\nu}$ for several systems with $80 < L < 180$, $W_c = 3.5$, $z = 1.43$ [Fig. 6]. The estimated correlation length exponent is $\nu_L = 1.1 \pm 0.1$. Thus, $\rho(0)$ displays a single-parameter scaling and serves as an order parameter across the WSM-CDM QPT.

Conclusions: To conclude we show that WSM is stable against weak disorder, but undergoes a QPT and becomes a CDM as the disorder is gradually increased. The double-WSM, on the other hand, becomes a CDM even for weak (infinitesimally small in the thermodynamic limit) disorder. The mean DOS at zero energy is shown to serve as the order parameter across the WSM-CDM itinerant QPT and display a single-parameter scaling. We also estimate the extend of the critical regime at finite energy associated with such QCP that can also be measured from ARPES experiments in various WSMs [6–10] and topological Dirac semimetals (two superimposed WSMs), such as Cd_2As_3 [39], Na_3Bi [40]. Within our numerical accuracy, the critical exponents (ν, z) appear to be independent of the number of Weyl nodes (N_W), which stem from the fact that contributions from *fermionic-bubble* vanish in the vanishing replica limit [25]. Generalizing the scaling analysis we find that weak disorder is a *relevant* perturbation in *triple-WSM* (monopole charge ± 3), since $[\Delta] = 1 - \frac{2}{n} = \frac{1}{3}$ when $n = 3$. Therefore, among various three-dimensional topological semimetals only the WSM is stable against weak disorder [41].

Acknowledgment: J. D. S. and B. R. were supported by the start up grant of J. D. S. from University of Maryland. We thank Max Planck Institute for Complex Systems, Dresden for hospitality during the workshop “Topology and Entanglement in Correlated Quantum Systems” (2014) where this work was initiated. We are thankful to S. Das Sarma, P. Goswami, I. F. Herbut, K. Imura, V. Jurićić, J. Pixley for valuable discussions.

-
- [1] M. Z. Hassan, C. L. Kane, *Rev. Mod. Phys.* **82**, 3045 (2010).
- [2] X. L. Qi, S.-C. Zhang, *Rev. Mod. Phys.* **83**, 1057 (2011).
- [3] B.-J. Yang, N. Nagaosa, *Nat. Commun.* **5**, 4898 (2014).
- [4] T. Morimoto, A. Furusaki, *Phys. Rev. B* **89**, 235127 (2014).
- [5] For review see, A. A. Burkov, *J. Phys.: Condens. Matter* **27**, 113201 (2015), and references therein.
- [6] C. Zhang, *et. al.*, arXiv:1502.00251.
- [7] S.-Y. Xu, *et. al.*, arXiv:1502.03807.
- [8] B. Q. Lv, *et. al.*, arXiv:1502.04684.
- [9] S.-Y. Xu, *et. al.*, arXiv:1504.01350.
- [10] N. Xu, *et. al.*, arXiv:1507.03983.
- [11] X. Wan, A. M. Turner, A. Vishwanath, and S. Y. Savrasov, *Phys. Rev. B* **83**, 205101 (2011).
- [12] A. A. Burkov, and L. Balents, *Phys. Rev. Lett.* **107**, 127205 (2011).
- [13] A. A. Zyuzin, S. Wu, and A. A. Burkov, *Phys. Rev. B* **85**, 165110 (2012).
- [14] C. X. Liu, P. Ye, and X. L. Qi, *Phys. Rev. B* **87**, 235306 (2013).
- [15] C. Fang, H. J. Gilbert, X. Dai, and A. B. Bernevig, *Phys. Rev. Lett.* **108**, 266802 (2012).
- [16] S.-M. Huang, *et al.*, arXiv:1503.05868.
- [17] E. Fradkin, *Phys. Rev. B* **33**, 3263 (1985).
- [18] R. Shindou, and S. Murakami, *Phys. Rev. B* **79**, 045321 (2009).
- [19] Y. Ominato, and M. Koshino, *Phys. Rev. B* **89**, 054202 (2014).
- [20] P. Goswami, and S. Chakravarty, *Phys. Rev. Lett.* **107**, 196803 (2011).
- [21] S. V. Syzranov, L. Radzihovsky, V. Gurarie, *Phys. Rev. Lett.* **114**, 166601 (2015); S. V. Syzranov, V. Gurarie, L. Radzihovsky, *Phys. Rev. B* **91**, 035133 (2015).
- [22] R. Nandkishore, D. Huse, S. L. Sondhi, *Phys. Rev. B* **89**, 245110 (2014).
- [23] Z. Huang, D. P. Arovas, A. V. Balatsky, *New J. Phys.* **15**, 123019 (2013).
- [24] B. Skinner, *Phys. Rev. B* **90**, 060202 (2014).
- [25] B. Roy, and S. Das Sarma, *Phys. Rev. B* **90**, 241112(R) (2014).
- [26] A. Altland, and D. Bagrets, *Phys. Rev. Lett.* **114**, 257201 (2015).
- [27] K. Kobayashi, T. Ohtsuki, K.-I. Imura, *Phys. Rev. Lett.* **110**, 236803 (2013).
- [28] K. Kobayashi, T. Ohtsuki, K.-I. Imura, I. F. Herbut, *Phys. Rev. Lett.* **112**, 016402 (2014).
- [29] B. Sbierski, G. Pohl, E. J. Bergholtz, P. W. Brouwer, *Phys. Rev. Lett.* **113**, 026602 (2014).
- [30] J. H. Pixley, P. Goswami, and S. Das Sarma, arXiv:1502.07778.
- [31] B. Sbierski, E. J. Bergholtz, P. W. Brouwer, arXiv:1505.07374.
- [32] J. H. Pixley, P. Goswami, and S. Das Sarma, arXiv:1505.07938.
- [33] C.-Z. Chen, J. Song, H. Jiang, Q.-F. Sun, Z. Wang, X. C. Xie, arXiv:1507.00128.
- [34] S. Liu, T. Ohtsuki, R. Shindou, arXiv:1507.02381.
- [35] See “Supplementary Materials” for tight-binding model and renormalization group analysis for double-WSM, analysis of critical exponents for WSM with $N_W = 4$.
- [36] A. Weiße, G. Wellein, A. Alverman, and H. Feshke, *Rev. Mod. Phys.* **78**, 275 (2006).
- [37] S. Sachdev, *Quantum Phase Transitions* (Cambridge University Press, 2nd ed., 2007).
- [38] I. F. Herbut, *A Modern Approach to Critical Phenomena* (Cambridge University Press, Cambridge, 2007).
- [39] S. Borisenko, Q. Gibson, D. Evtushinsky, V. Zabolotnyy, B. Buechner, and R. J. Cava, *Phys. Rev. Lett.* **113**, 027603 (2014).
- [40] Z. K. Liu, *et. al.*, *Science*, **343**, 864 (2014).
- [41] P. Goswami, *unpublished*.

Supplementary Materials for “*Dirty Weyl semimetals: stability, phase transition and quantum criticality*”

In this Supplementary material, we provide some additional details of (i) tight-binding model for double-WSM, (ii) display the renormalization group flow equation of disorder couplings in double-WSM, and (iii) present the numerical analysis for WSM with $N_W = 4$.

• *Tight-binding model for double-WSM*: As announced in the main part of the paper by setting $N_1(\mathbf{k}) = t_1[\sin(k_1a) - \sin(k_2a)]$, $N_2(\mathbf{k}) = t_1 \cos(k_1a) \cos(k_2a)$, $N_3^1(\mathbf{k}) = t \cos(k_3a)$ and $N_3^2(\mathbf{k}) = t'[2 - \cos(k_1a) - \cos(k_2a)]$ in Eq. (1), one can realize a double-WSM in the vicinity of $\mathbf{k} = (\frac{\pi}{2a}, \frac{\pi}{2a}, \pm\frac{\pi}{2a})$. In cubic lattice with periodic boundary in each direction, the corresponding tight-binding model is

$$H = \sum_{\mathbf{r}} \left[\frac{t}{2} \Psi_{\mathbf{r}}^\dagger \sigma_3 \Psi_{\mathbf{r}+\hat{e}_3} + \frac{it}{2} [\Psi_{\mathbf{r}}^\dagger \sigma_1 \Psi_{\mathbf{r}+\hat{e}_1} - \Psi_{\mathbf{r}}^\dagger \sigma_1 \Psi_{\mathbf{r}+\hat{e}_2}] + \frac{t}{4} \sum_{\alpha=\pm} \Psi_{\mathbf{r}+\hat{e}_1}^\dagger \sigma_2 \Psi_{\mathbf{r}+\alpha\hat{e}_2} - \frac{t'}{2} \sum_{j=1,2} \Psi_{\mathbf{r}}^\dagger \sigma_3 \Psi_{\mathbf{r}+\hat{e}_j} + H.c \right] + \sum_{\mathbf{r}} \Psi_{\mathbf{r}}^\dagger [2t' \sigma_z + V(\mathbf{r})] \Psi_{\mathbf{r}}, \quad (8)$$

where $\Psi_{\mathbf{r}}$ is a two-component spinor defined in the main text. $V(\mathbf{r})$ captures the effect of random quenched charge impurities.

• *RG analysis for double-WSM*: While the scaling analysis suggest that disorder is a marginal perturbation in double-WSM, to establish that weak disorder is marginally relevant one needs to account for the quantum (loop) corrections. The replicated action (imaginary time) reads as

$$\bar{S} = \int d^3x dt \Psi_a^\dagger [\partial_t + \sigma_1 \frac{\partial_2^2 - \partial_1^2}{2m} - \sigma_2 \frac{2\partial_1\partial_2}{2m} - iv\tau\sigma_3\partial_z] \Psi_a(x, t) - \frac{\Delta}{2} \int d^3x dt dt' (\Psi_a^\dagger \Psi_a)_{(x,t)} (\Psi_b^\dagger \Psi_b)_{(x,t')} - \frac{\Delta_\perp}{2} \sum_{j=1,2} \int d^3x dt dt' (\Psi_a^\dagger \sigma_j \Psi_a)_{(x,t)} (\Psi_b^\dagger \sigma_j \Psi_b)_{(x,t')}, \quad (9)$$

Here we have introduced a new disorder coupling Δ_\perp , since the renormalization group flow equations cannot be closed in terms of one coupling constant Δ (as shown below). However, the new coupling (Δ_\perp) does not change the announced outcome. Upon integrating out the fast Fourier modes with $\Lambda e^{-l} < \sqrt{\left(\frac{k_\perp^2}{2m}\right)^2 + v^2 k_z^2} < \Lambda$, where Λ is the ultraviolet cut-off, we arrive at the following renormalization group (RG) flow equations

$$\frac{d\Delta_0}{dl} = \Delta_0^2 + \Delta_\perp^2 + 3\Delta_0\Delta_\perp, \quad \frac{d\Delta_\perp}{dl} = \frac{1}{2} (\Delta_0^2 + 3\Delta_\perp^2 + \Delta_0\Delta_\perp), \quad (10)$$

after taking $\Delta m/(2\pi v) \rightarrow \Delta$, $\Delta_\perp m/(2\pi v) \rightarrow \Delta_\perp$, at the one-loop level. The above set of flow equations supports only one *unstable* fixed point at $(\Delta_0, \Delta_\perp) = (0, 0)$. Thus weak disorder is a marginally relevant perturbation in double-WSM and drives the system into the CDM phase. Notice that here we considered only the intra-valley disorder potentials. For Anderson transition one needs to account for the inter-valley disorders as well. However, inclusion of such additional channels do not alter the stability of ballistic fermions in double-WSM at weak disorder.

• *Numerical analysis for WSM with $N_W = 4$* : Finally, we present the numerical analysis for W_c (critical disorder for WSM-CDM transition), and various critical exponents (ν and z) in WSM with $N_W = 4$. The results are already quoted in Table I of main part of the paper. These quantities are extracted by using identical methods as described in the main paper. Thus, here we present the corresponding figures, analogous to the ones in Fig. 3 (for $N_W = 1$) of the paper.

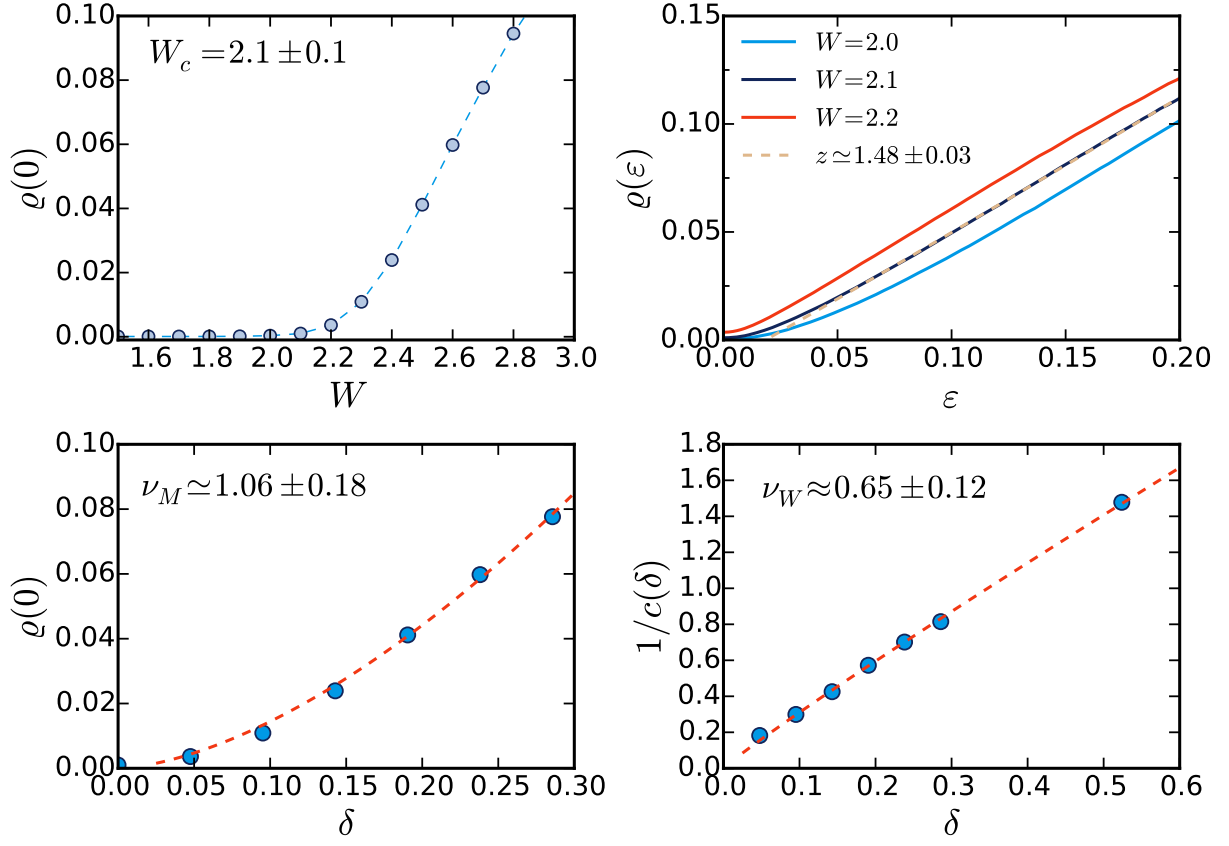


FIG. 7. (Color online) (a) Mean DOS at zero energy $\rho(0)$ vs. disorder (W), (b) mean DOS $\rho(\varepsilon)$ vs. ε for $W = 2.0, 2.1, 2.2$, (c) $\rho(0)$ vs. δ , where $\delta = (W - W_c)/W_c$, and (d) $c(\delta)^{-1}$ vs. δ , where $c(\delta) = \delta^{(z-1)\rho(\delta)}$, for WSM with $N_W = 4$. Extracted values of W_c , z and ν are quoted in Table I.